Tropical Cyclone Climatology in a Global-Warming Climate as Simulated in a 20 km-Mesh Global Atmospheric Model: Frequency and Wind Intensity Analyses

Kazuyoshi OOUCHI

Advanced Earth Science and Technology Organization, Earth Simulator Center, Yokohama, Japan

Jun YOSHIMURA, Hiromasa YOSHIMURA

Meteorological Research Institute, Tsukuba, Japan

Ryo MIZUTA

Advanced Earth Science and Technology Organization, Tsukuba, Japan

Shoji KUSUNOKI and Akira NODA

Meteorological Research Institute, Tsukuba, Japan

(Manuscript received 30 April 2005, in final form 15 November 2005)

Abstract

Possible changes in the tropical cyclones in a future, greenhouse-warmed climate are investigated using a 20 km-mesh, high-resolution, global atmospheric model of MRI/JMA, with the analyses focused on the evaluation of the frequency and wind intensity. Two types of 10-year climate experiments are conducted. One is a present-day climate experiment, and the other is a greenhouse-warmed climate experiment, with a forcing of higher sea surface temperature and increased greenhouse-gas concentration. A comparison of the experiments suggests that the tropical cyclone frequency in the warm-climate experiment is globally reduced by about 30% (but increased in the North Atlantic) compared to the present-day-climate experiment. Furthermore, the number of intense tropical cyclones increases. The maximum surface wind speed for the most intense tropical cyclone generally increases under the greenhouse-warmed condition (by 7.3 m s^{-1} in the Northern Hemisphere and by 3.3 m s^{-1} in the Southern Hemisphere). On average, these findings suggest the possibility of higher risks of more devastating tropical cyclones across the globe in a future greenhouse-warmed climate.

Corresponding author: Kazuyoshi Oouchi, Advanced Earth Science and Technology Organization (AESTO), MRI Group, 3rd Floor, c/o Research Exchange Group, Earth Simulator Center, 3173-25 Showa-machi, Kanazawa-ku, Yokohama 236-0001, Japan.
E-mail: kouchi@mri-jma.go.jp

1. Introduction

To understand the possible changes in tropical cyclones in a greenhouse-warmed world remains a high priority issue from both scientific and socio-economic viewpoints. Studies on this issue have been undertaken with global climate models (e.g., Broccoli and Manabe 1990; Haarsma et al. 1993; Bengtsson et al. 1996; Krishnamurti et al. 1998; Sugi et al. 2002; Tsutsui 2002; Yoshimura et al. 2005) and regional nested models (e.g., Knutson et al. 1998; Knutson and Tuleya 1999, 2004; Walsh and Ryan 2000). Among the problems frequently discussed, the possible changes in the frequency and intensity of future tropical cyclones are more relevant to the present study. With a high-resolution regional model (using a 1/6 degree mesh at the innermost area in a triply nested model), Knutson et al. (1998) studied the tropical cyclones in the northwest Pacific under a CO_2-induced warming condition and reported that the model simulated significantly stronger hurricane intensities in a high-CO_2 environment (in which the surface wind increases by 3–7 m s^{-1} from the present-day climate condition). The finding was consistent with the "theoretical prediction" from a potential intensity theory proposed by Emanuel (1987) and, alternatively, by Holland (1997). On the other hand, the prediction of the frequency change of tropical cyclone in a greenhouse-warmed climate has yielded mixed results even regarding the signs of change.

The results from most of these studies with global models, however, have left room for further investigation, mainly because a typical resolution of 100 kilometers was too coarse to represent the typical inner structures (e.g., mesoscale convection) of a tropical cyclone (Krishnamurti et al. 1989). Although we can infer that coarse-resolution climate models are adequate for introducing some dynamical large-scale constraints on the tropical cyclone climatology as needed in the real atmosphere, it is inadequate for elaborated and accurate forecast of tropical cyclone intensity. Such a model may create tropical disturbances that could satisfy given identification criteria (Camargo and Sobel 2004). Even if enough fine resolution is employed with a regional-nesting technique, the characteristics of the tropical cyclones on a global, climate scale will usually not be investigated due to limited computational resources.

Now that the Earth Simulator (Sato 2004) is operating, a high-resolution, global climate model can be used to clarify the problem. The advantage of high resolution is that the model is capable of representing a tropical cyclone both as an ensemble of mesoscale convective systems and as a synoptic scale disturbance, which is developed as a result of its spontaneous (not artificially forced) interaction with the environmental disturbances within a climate system. Therefore, the use of the 20 km-mesh model will provide more reliable information concerning how the greenhouse-warmed climate would affect a tropical cyclone than that from previous studies that relied on climate models with a coarser resolution. This article reports the main findings of the problem.

On the other hand, this study also reveals that the downscaling of the grid size alone does not address all the issues relating to the projection of future tropical cyclones. Obviously, the physical parameterizations in the model must be refined to increase the reliability of the projection. This study is expected to serve as a step toward that goal given that some uncertainty coming from the coarse-resolution of the traditional model is excluded to some extent by using a 20 km mesh. The issue is discussed in more detail in Section 4.

This paper is organized as follows. An overview of the model and experimental setup is provided in Section 2, which is followed by a presentation of the simulated results in Section 3. The article is concluded with a discussion and interpretation of the results in Section 4, which contains comparisons of the obtained results with those obtained by past modeling studies on tropical cyclone projections.

2. Methodology

2.1 Overview of the model and numerical experiments

The tropical cyclone projection discussed in this paper is based on the outputs from two sets of 20 km-mesh, high-resolution AGCM experiments carried out on the Earth Simulator. The details of the model and the experiments are described in Kusunoki et al. (2005) and Mizuta et al. (2006). Briefly, the 20 km-mesh

model is a Meteorological Research Institute (MRI)/Japan Meteorological Agency (JMA) unified model originated from the operational numerical weather prediction model, with some modifications for a climate research objective (Mizuta et al. 2006). The time integration was accelerated with the introduction of a vertically conservative semi-Lagrangian scheme (Yoshimura and Matsumura 2003; Yoshimura and Matsumura 2005), which allows nearly 4 hours of wall-clock time for a 1-month time integration with a time step of 360 seconds by using 30 nodes of the Earth Simulator. The model is configured with the horizontal spectral truncation of TL959 (equivalent to about 20 km mesh), and 60 vertical levels with the model top at 0.1 hPa. The cumulus parameterization used is a prognostic Arakawa-Schubert scheme (Randall and Pan 1993; Arakawa and Schubert 1974).

To obtain a reasonable performance of the 20 km-mesh climate model, careful tuning of the physical processes was needed. Our strategy in the tuning was to keep, or improve the quality of the climatological representation in the original coarser-mesh version, while making the representation of convection associated with a tropical cyclone more realistic (Mizuta et al. 2006). It turned out that the manner of the organization of convection into a tropical cyclone critically depends upon the amount of cumulus momentum transport in the momentum transport parameterization used. To make it more realistic, the transport amount, which is tunable by an adjustment parameter, was reduced by about 40% compared to the original coarser-mesh version at T106 (equivalent to about 120 km mesh). The details will be found in Mizuta et al. (2006).

The experiments follow the so-called "time-slice" method (Bengtsson et al. 1996; IPCC 2001). First, a 10-year present-day experiment was conducted with the forcing of the observed climatological sea surface temperature (SST) average from 1982 to 1993. Next, an SST change between the future (average over 2080–99) and the present (average over 1979–98) experiments was added onto the observed SST. The SST change was predicted by the MRI-CGCM2.3 (Yukimoto et al. 2006) on the basis of the IPCC A1B emission scenario (IPCC 2000) with the CO_2 concentration nearly doubled around the 2080–99 period, and the global mean surface air temperature rising by 2.5 degrees. Under the SST condition, the model was integrated over 10 years as a future global-warmed climate experiment. In the future experiment, the concentrations of greenhouse gas and the aerosols are taken from the values of the year 2090 in the A1B scenario.

2.2 Tropical cyclone identification method

This study focuses on elucidating the differences of tropical cyclone climatology between the present-day climate condition and a future, greenhouse-warmed climate condition derived from the respective 10-year time integration period. The differences in the tracks (geographical distributions), maximum wind speed are the targets of our comparison. The data size of the default, 20 km-mesh output including the basic meteorological elements of the dynamical and thermodynamical physical quantities, amounts to about 60 GB per month. Due to the difficulties in handling such an enormous dataset in an encompassing manner, we were forced to carefully select only relevant output parameters featuring the tropical cyclones. In addition, considering also the versatile aims of the current numerical experiments (Mizuta et al. 2006; Kusunoki et al. 2005), only a limited number of output variables, but minimizing scientific compromises, were allowed in the tropical cyclone analysis.

To identify tropical cyclones from the outputs of the present-day and future experiments, we applied the following method and criteria: the target area was specified between 45 S and 45 N latitudinal belts over the ocean. The initial position of each tropical cyclone was limited to the region between 30 S and 30 N. Over the specified area, the tropical cyclones were searched with the following 6 sets of criteria, which are basically the same as those used by Sugi et al. (2002) and originally in line with those of Bengtsson et al. (1996).

(1) Across the 45 S–45 N latitudinal belt, the grid point corresponding to a TC-center candidate was defined as the one where the minimum surface pressure is at least 2 hPa lower than the mean surface pressure over the surrounding 7 degree $\times$ 7 degree grid box.

(2) The magnitude of the maximum relative vorticity at 850 hPa exceeds 3.5×10^{-5} s^{-1}.
(3) The maximum wind speed at 850 hPa is larger than 15 m s^{-1}.
(4) The temperature structure aloft has a marked warm core such that the sum of the temperature deviations at 300, 500 and 700 hPa exceeds 2 K.
(5) The maximum wind speed at 850 hPa is larger than that at 300 hPa.
(6) The duration is not shorter than 36 hours.

Criteria (2)–(6) were applied to the region near the tropical cyclone center candidate satisfying criterion (1). The relevant physical properties of the tropical cyclones satisfying all the criteria were saved every 6 hours for the analyses presented in this article. Concerning criterion (3), the use of surface wind with the thershold of 17 m s^{-1} turned out to be too stringent for simulating the observed annual frequency of tropical cyclones. The use of a 15 m s^{-1} threshold in criterion (3) is simply intended to make the model-produced tropical cyclone frequency comparable to the observed annual frequency (about 80 TCs per year). In fact, about 62.7% of the tropical cyclones simulated in the present-day experiment have a maximum surface wind speed of more than 17 m s^{-1}. This demonstrates a reasonable model performance for simulating a tropical cyclone. In the analyses presented in this article, surface wind speed defined at 10 m height is used unless otherwise stated. Concerning criterion (4), a possible global-warming-driven change in the warm-core structure itself merits investigation, but is beyond the scope of this article. Relevantly, one of the coauthors happened to have an opportunity to check the influence of the warm-core criterion upon the tropical cyclone frequency projected in a T106 version of a global model, by increasing a threshold of the vertically cumulative temperature anomaly. The result showed that the tropical cyclone frequency remained almost unchanged for the intense events (minimum surface pressure of, for example, less than 1,000 hPa). Criterion (5) is intended to remove extratropical cyclones.

2.3 The observational dataset for the output verification

To verify the simulated tropical cyclone climatology, a global tropical cyclone data set obtained from the website of the Unisys Corporation is used; the data set combines the "best track" tropical cyclone data sets from the National Hurricane Center (NHC) of the U.S. National Oceanic & Atmospheric Administration, and from the U.S. Joint Typhoon Warning Center (JTWC). The NHC data set contains tracks for the North Atlantic and the eastern North Pacific basins. The JTWC data set contains tracks for the western North Pacific Ocean, the North Indian Ocean, and the Southern Hemisphere. Out of the dataset, we retrieved the dataset of the 1979–1998 period, with the maximum surface wind speed at 17.2 m s^{-1} (34 kt) or higher for our analyeses.

3. Results

3.1 An example of a tropical cyclone rainfall morphology

Compared to previous climate models with a coarser mesh, an advantage of using the 20 km-mesh model is the improvement in the representation of the inner structures of a tropical cyclone. To gain insight into some morphological aspects of the improvement, a typical tropical cyclone in the present-day experiment is shown in Fig. 1. The figure illustrates (a) the 6-hour averaged rainfall amount over a western North Pacific region near Japan, (b) the 6-hour averaged rainfall amount near a tropical cyclone in the mature stage, (c) a temperature anomaly at 925 hPa as a deviation from the displayed area mean, (d) the water vapor mixing ratio at 925 hPa, and (e) the velocity at 925 hPa. The area displayed in panels (d) and (e) is an expanded view of the area surrounded by thick-dashed lines in panel (b). In panels (d) and (e), the distribution of the precipitation is also plotted with white contours.

Figure 1a demonstrates that the 20 km-mesh model reproduces a variety of precipitation features, with wide-ranging scales and a hierarchy, including a remnant of the precipitation from a frontal system stretching across the Pacific coastal region of Japan, a tropical cyclone on its way to Japan, and some organized cloud ensembles located to the south of the tropical cyclone. In the following, the typical hierarchy of the simulated precipitation features in the tropical cyclone is described. In Fig. 1b, it is evident that a comma-shaped stronger rainfall region, labeled A, spreads immediately outside

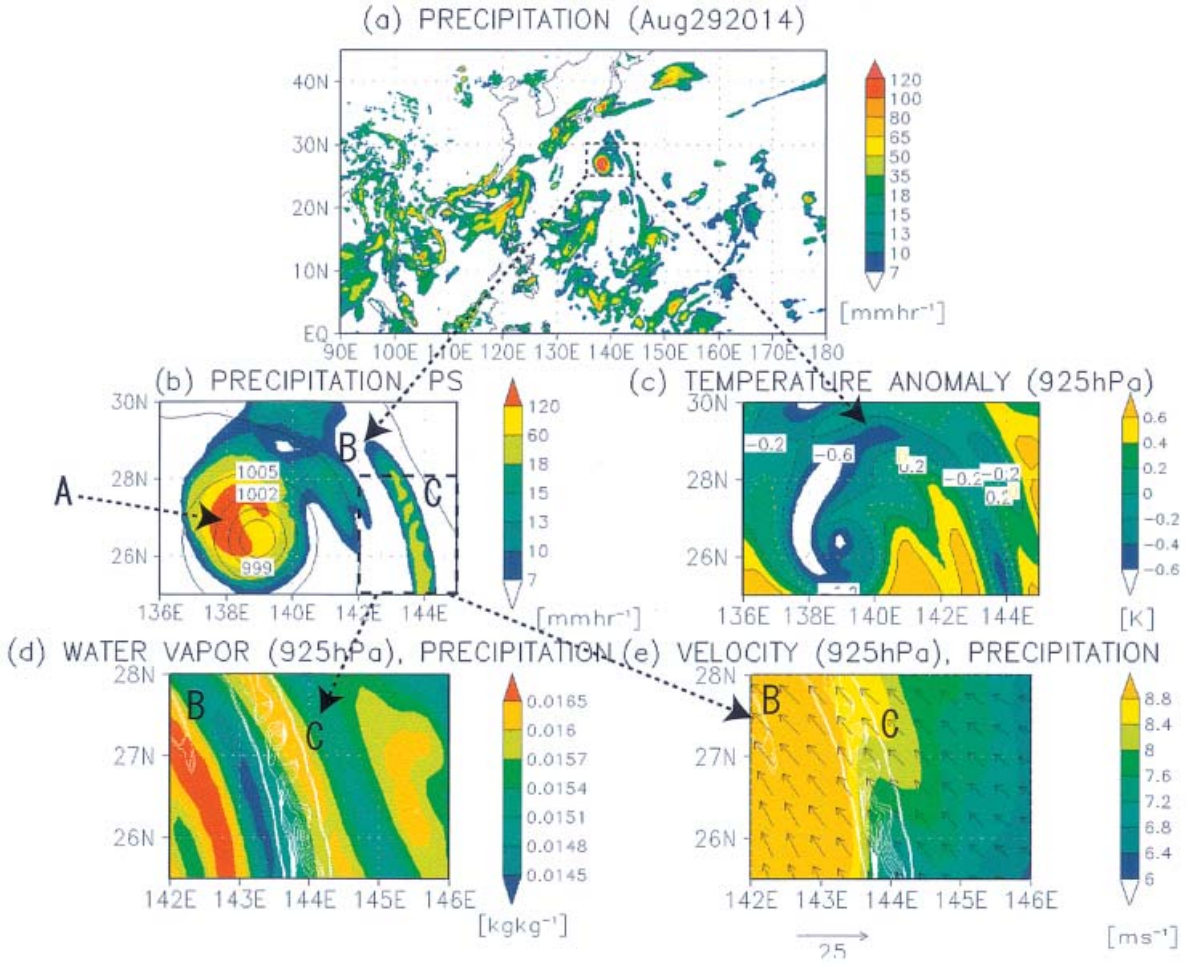

Fig. 1. Horizontal view of a tropical cyclone simulated in the present-day experiment (Aug 29, 7th year of the time integration): horizontal distributions of (a) 6-hour averaged precipitation amount in mm hour^{-1} in the near-Japan, and northwest Pacific region. The rest of the panels focus on a tropical cyclone, displaying (b) 6-hour averaged precipitation amount in mm hour^{-1} (shaded) and surface pressure (contour), (c) temperature anomaly at 925 hPa in K, (d) water vapor mixing ratio at 925 hPa in kg kg^{-1} (shaded) and precipitation amount (white contour), and (e) horizontal velocity at 925 hPa in m s^{-1} (shaded and arrows) and precipitation amount in mm hour^{-1} (white contour). The domain of panel (d) and (e) is an expanded view of the region surrounded by a dotted box in panel (b).

of the lowest surface pressure region. Region A may be likely to correspond to the eyewall of the tropical cyclone. In the northeastern to eastern quadrant of the lowest pressure center, spiral-form rainbands B and C are present. Although not shown, an examination of the time sequence of B and C reveals that the rainbands, as they develop, move inward so as to eventually merge into the innermost eyewall area. Although the present 20 km-mesh global model does not incorporate any sophisticated cloud micro-physics to allow a full-scale comparison of the simulated behaviors of the rainbands with the observations, it can be inferred that, in the organization and maintenance of B and C, some meso-beta scale thermodynamical processes are at work, even if not as elaborately as in nonhydrostatic tropical cyclone models. In Fig. 1c, conspicuous negative temperature anomalies coincide with the stronger rainfall

regions corresponding to A, B, and C. These negative anomalies may partly originate from the evaporation of the rainwater from A, B, and C. At the eastern edge of rainband C, the boundary layer is relatively moist (Fig. 1d), and the low-level flow is from the southeast (Fig. 1e). These conditions may be favorable for the maintenance of rainband C. It is interesting to note that rainband C is represented not as a homogeneous rainfall area, but as an ensemble of substructures with varying rainfall intensity. The substructures are indicative of cellular convective structures, which are embedded in observed tropical cyclone rainbands (e.g., Willoughby et al. 1984). Thus, the typical inner structure of a tropical cyclone is captured more reasonably compared to the previous coarser-mesh climate models, in which the representation of the inner structure, including the eye, has been somewhat elusive (Krishnamurti et al. 1989). In order to achieve a realistic simulation of the inner structures, the model should be improved. To further explore the reliability of the "inner structure," we need to clarify the validity of the cumulus parameterization used. Although the problem itself merits investigation, it is beyond the scope of this article and will be examined in a future study. Within the present purpose of investigating the tropical cyclone climatology, the simulated inner structure of a tropical cyclone provides an important improvement over those in previous studies.

3.2 Tracks and geographical distribution

Figure 2 shows the tropical cyclone tracks simulated over the 10-year integration period of present-day (middle) and future (low) experiments, together with the best tracks of the observational global tropical cyclone dataset from 1979 to 1998 (upper). The tracks for the present-day experiment, which are in general agreement with the observation, reveal that the 20 km-mesh model succeeds in representing the geographical distributions reasonably well.

Nevertheless, there are some inconsistencies between the results of the observation and those of the model result. Most noticeably, there is a deficiency in the occurrence in and around the model western Pacific region. The model tropical cyclones tend to be generated more to the north of the observed locations. The deficiency may be partly relevant to a weaker bias of the precipitation amount in this region compared to the observations (Mizuta et al. 2006). The model's inability to sufficiently represent the horizontal precipitation distribution in the subtropical western Pacific was common to most of the climate models, as revealed from an AMIP type intercomparison study (Kang et al. 2002).

Another inconsistency is evident in the south Indian Ocean, where the observed tropical cyclones generally occur outside the 0–10 S latitudinal belt; however, this is not the case in the model results. Though there is a case in which a tropical cyclone is observed near the equator (Chang et al. 2003), the current model obviously overpredicts the generation of tropical cyclones at very low latitudes. A similar "equatorward bias" in the tropical cyclone formation was also found in other global climate models with coarser horizontal resolution (e.g., at T42∼2.8 degree in Camargo et al. 2005). Camargo et al. (2005) inferred that the bias may originate from insufficient resolution of the model, which may dilute some dynamical processes that are otherwise to be shared among finer adjacent grid boxes. As our model has relatively higher resolution at 20 km, we may need to explore other possibilities. Our model also has a bias to predict many more tropical cyclones around the dateline than in the observations. Moreover, the tracks for the present-day experiment indicate a small but nonnegligible number of tropical cyclones off the coast of Brazil, which was recently pointed out from an observational study (Pezza and Simmonds 2005). To explain the discrepancy between the model results and observations, we would need to scrutinize additional cases, by extending our analysis into datasets containing other years. These shortcomings need to be ameliorated to achieve a more accurate prediction of the geographical distribution of tropical cyclones. A general comparison between the present-day and future experiments indicates that the geographical distribution of tropical cyclones would not be altered significantly under the greenhouse-warmed condition, supporting what has been inferred and projected from previous studies (Haarsma et al. 1993; Bengtsson 2001).

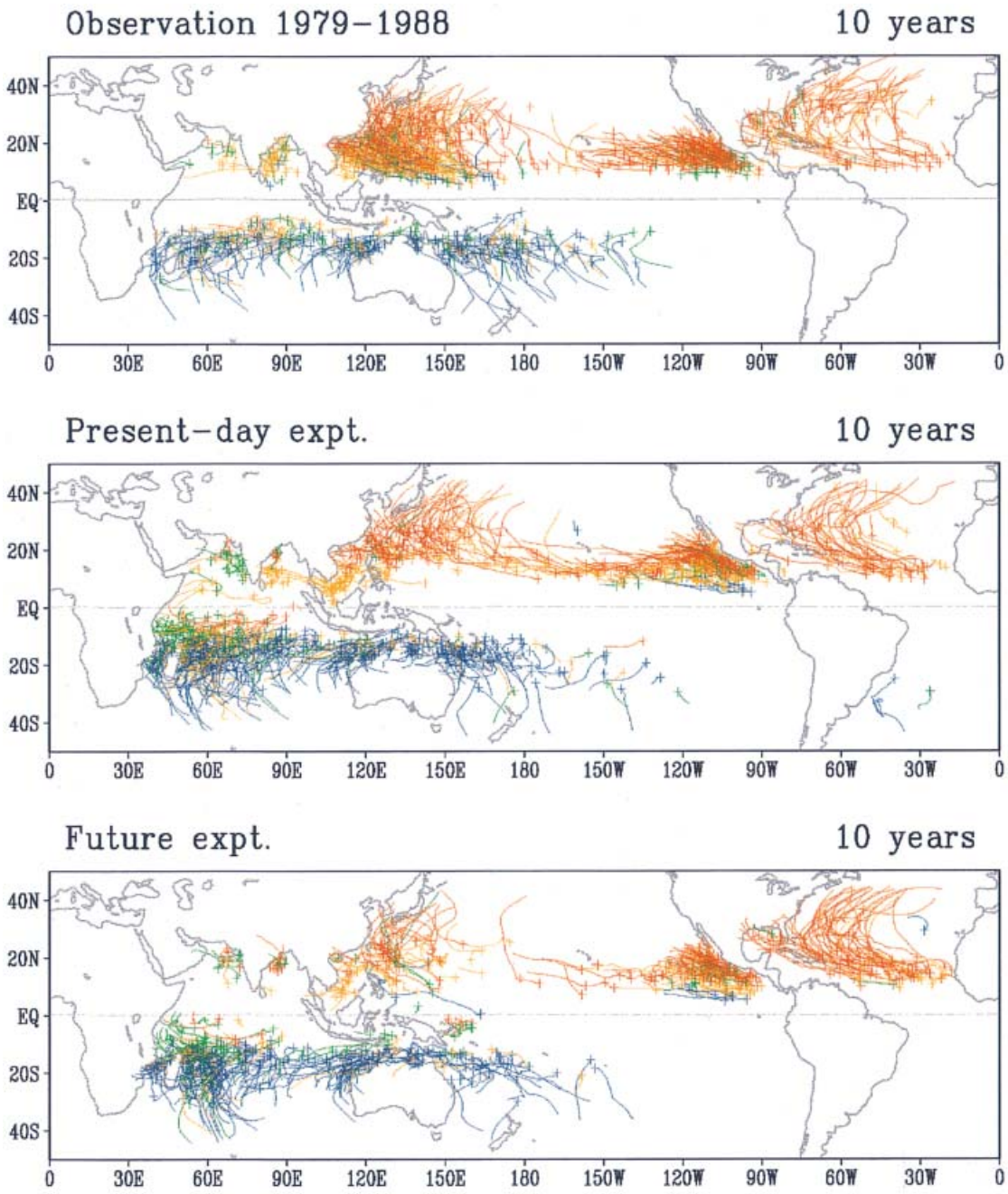

Fig. 2. Tropical cyclone tracks of the observational data (top), the present-day (middle), and the future climate experiments (bottom). The initial positions of tropical cyclones are marked with "plus" signs. The tracks detected at different seasons of each year is in different colors (blue for January, February, and March; green for April, May, and June; red for July, August, and September; orange for October, November, and December).

3.3 Frequency

In Fig. 2, it is evident that the frequency of tropical cyclones is reduced in the future experiment compared to the present-day experiment, as may be noted in the differences in the density of the tracks. The tropical cyclone frequency investigated region-wise is indicated in Table 1, where the annual-mean numbers of tropical cy-

Table 1 Frequency of tropical cyclone occurrence in the observational dataset and in the present-day and the future experiments. The annual-mean numbers are shown for the globe, the Northern and Southern Hemispheres, and six ocean basins (conveniently defined based on the latitudes and longitudes indicated in the table). Standard deviations are shown in parentheses. The two-sided Student's *t*-test was applied to the differences between the values from the present-day experiment and those from the future experiment.

Number of TCs	Latitudes	Longitudes	Observation 20 years	Present 10 years	Future 10 years
Global	45 S–45 N	ALL	83.7 (10.0)	78.3 (8.4)	54.8 (8.4)**
Northern Hemisphere	0–45 N	ALL	58.0 (7.1)	42.9 (7.0)	30.8 (5.8)**
Southern Hemisphere	0–45 S	ALL	25.7 (5.6)	35.4 (3.8)	24.0 (6.1)**
North Indian Ocean	0–45 N	30 E–100 E	4.6 (2.4)	4.4 (2.5)	2.1 (1.7)**
Western North Pacific Ocean	0–45 N	100 E–180	26.7 (4.2)	12.4 (3.7)	7.7 (2.6)**
Eastern North Pacific Ocean	0–45 N	180–90 W	18.1 (4.8)	20.5 (3.4)	13.5 (5.7)*
North Atlantic Ocean	0–45 N	90 W–0	8.6 (3.6)	5.6 (2.7)	7.5 (1.8)#
South Indian Ocean	0–45 S	20 E–135 E	15.4 (3.8)	25.8 (3.0)	18.6 (5.1)**
South Pacific Ocean	0–45 S	135 E–90 W	10.4 (4.0)	9.4 (3.3)	5.4 (1.9)**

** Statistically significant decrease at 99% confidence level.
* Statistically significant decrease at 95% confidence level.
# Statistically significant increase at 95% confidence level.

clones are shown for the globe, the Northern and Southern Hemispheres, and six ocean basins. The ocean basins were defined based on the latitudes and longitudes indicated in the table. In Table 1 (and Table 2 as explained later), a two-sided Student's *t*-test was applied to the differences between the values from the present and future experiments. In the test, storm results were aggregated for each year over each given region that constitute sample elements of the test for present (10 years) and future (10 years) experiments ($n1 = n2 = 10$). In the present-day experiment, the annual mean number (78.3) is almost comparable to the observation (83.7). In the future experiment, the annual mean number is reduced to 54.8, which is nearly a 30% reduction from the present-day experiment.

In the North Indian Ocean, Eastern North Pacific, North Atlantic, and Southern Pacific, the model has reasonably simulated the observed frequency and distribution of tropical cyclones. On the basin-wise scale, the model is, despite its high resolution, incapable of capturing the observed frequency in some basins: in the western North Pacific, the model underpredicts the number of the observed frequency for the tropical cyclone of any intensity class, as also inferred from the frequency deficiency in that region reported in 3.2; in the South Indian Ocean, on the other hand, the relative numbers are practically reversed, and the model overpredicts the number of observed frequency. In general, the model tends to overestimate/underestimate the occurrence number in the Southern/Northern Hemisphere.

A comparison between the future and present-day experiments reveals that the occurrence number in the future experiment is generally reduced, showing approximately 30% total global reduction, as stated before. The reduction trend remains evident across the Northern Hemisphere, Southern Hemisphere, North Indian Ocean, western North Pacific, South Indian Ocean, and South Pacific, at the 99% level of statistical significance (based on the two-sided Student's *t*-test). On the other hand, a tendency of increase in the future experiment is found in the North Atlantic Ocean, where the occurrence number increases by about 30%. Though the reason for this contrast in the tendency is not presently clear, a clue may be obtained by investigating the change in the sea surface temperature (SST) between the two experiments. The upper panel of Fig. 3 shows the difference of the SST between the

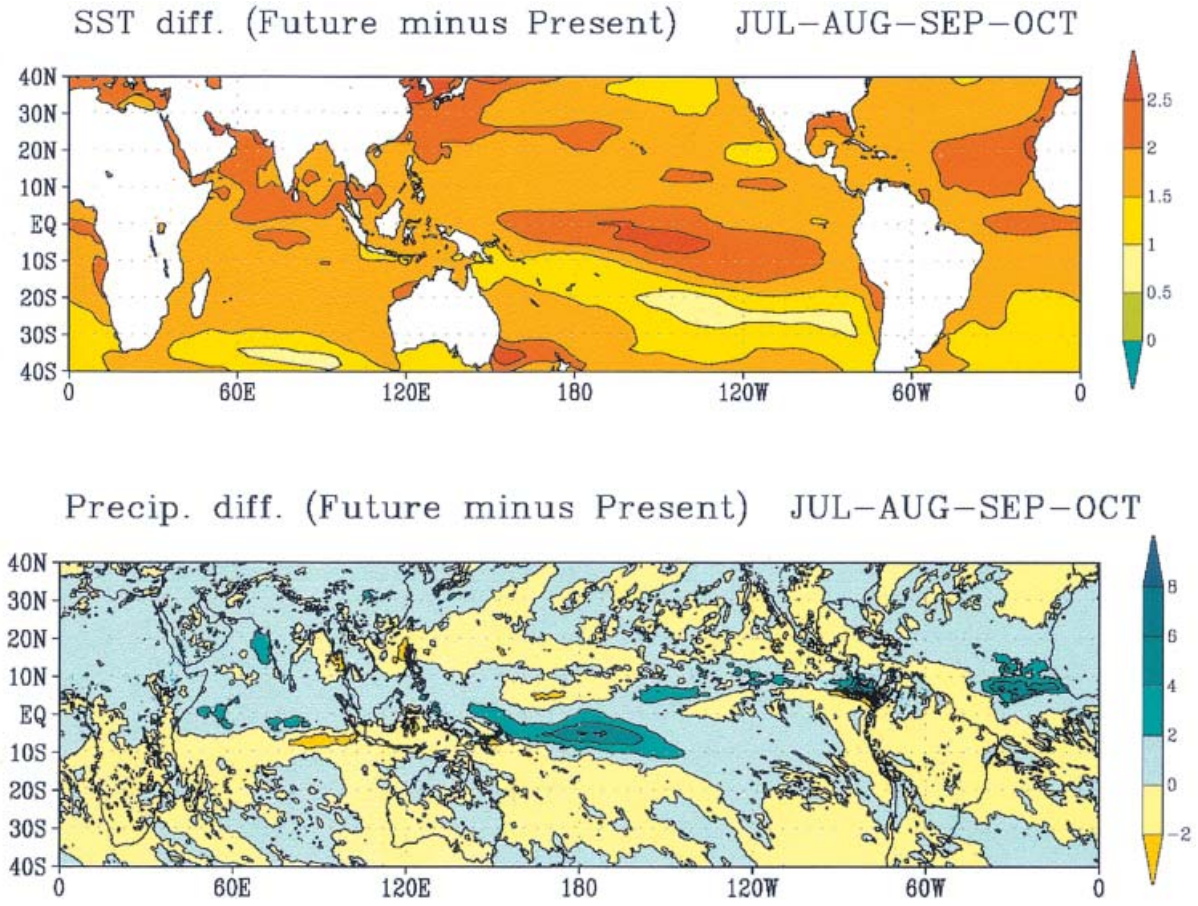

Fig. 3. Difference between the future and the present-day experiments (future minus present-day) in the sea surface temperature (upper) and precipitation amount (lower) derived from the average in the boreal tropical-cyclone season (July, August, September, and October) for the entire integration years.

experiments ("future minus present-day") as calculated from the average over the boreal summer months of the tropical cyclone season (July, August, September, October), while the lower panel displays the mean precipitation difference between the experiments. We can see that a positive region of SST spreads over the south-eastern part of the North Atlantic Ocean. The region approximately corresponds to the area of generation for most of the hurricanes that approach and threaten the eastern coast of the United States. Of the several signatures of such warm tongues over the globe, the one over the North Atlantic is conspicuous in size, and, more importantly, coincides with the tropical cyclone source. In addition, the accompanied difference in the rainfall amount, which is shown in the lower panel of Fig. 3, exhibits a trend of increase, indicative of activated convection. This should help "seed" the tropical cyclone generations. These features can be responsible for the increased frequency of tropical cyclones over the North Atlantic Ocean.

3.4 Intensity

The simulated reduction in the number of future tropical cyclones may be a positive sign from a socio-economic viewpoint; however, a concern is the increased devastation of tropical cyclones in a greenhouse-warmed world. A clue to answer the problem may be obtained by examining the simulated maximum surface wind speeds of the tropical cyclones, which are shown in Fig. 4. The annual mean numbers

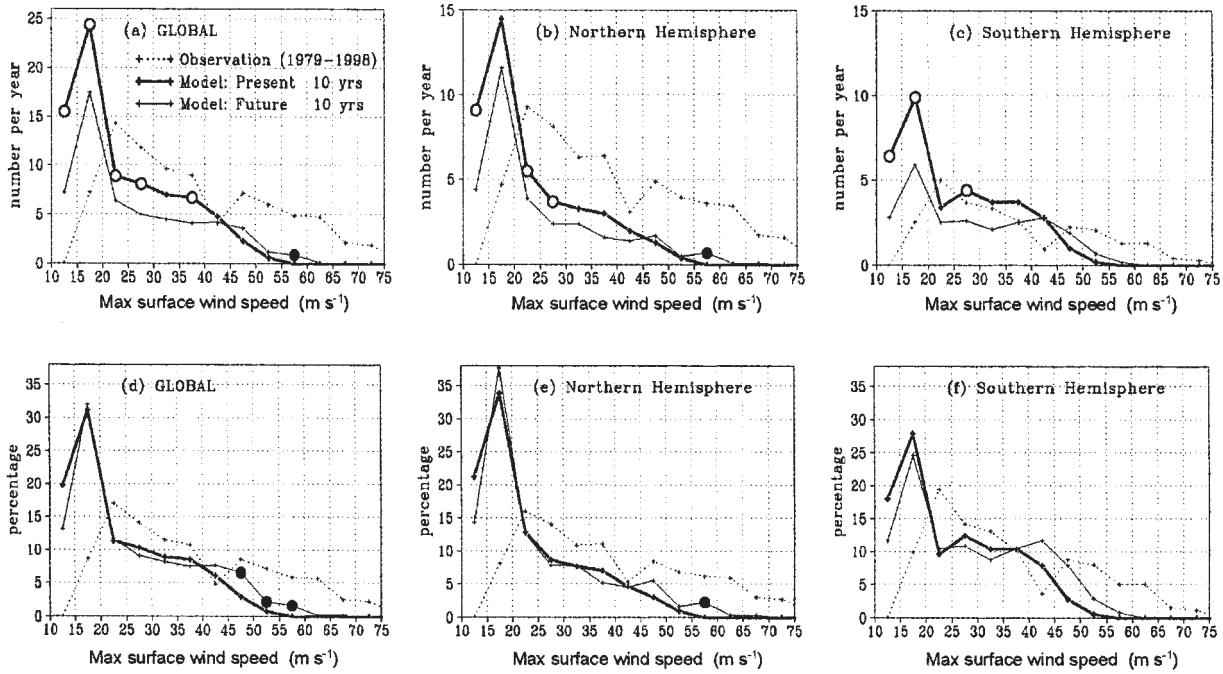

Fig. 4. (a, b, c) Annual mean occurrence frequency, (d, e, f) Occurrence rate (%) normalized by the total number of simulated tropical cyclones counted in the region specified as functions of the tropical cyclone intensities (abscissa) for (a, d) global, (b, e) Northern Hemisphere, and (c, f) Southern Hemisphere. The abscissa is the largest maximum surface wind speed, and the maximum wind speed attained in the lifetime of a tropical cyclone is plotted. Dotted lines indicate the observation; results from the present-day experiment are shown by thick solid lines, and those from the future experiment, by thin solid lines. For the difference between the "present" and "future" results, the plot at the 95% statistical significance level is marked with an open or closed circle (according to a two-sided Student's t-test). Note that plots from the observation include no tropical cyclone with the maximum surface wind speed at less than 17.2 m s^{-1}.

of the simulated tropical cyclones for the "present-day (thick solid lines)" and "future (thin solid lines)" experiments are plotted against the observation (dotted, black). In Fig. 4, a two-sided Student's t-test was applied to the difference between the "present" and "future" curves, to check the statistical significance. In deriving the significance level, storm results aggregated for the entire storm season each year were used as the sample elements of the t-test ($n1 = n2 = 10$, for each 10 years time integration). The segment of the graphs satisfying 95% significance level are marked with open and closed circles. The circles on thin/thick lines denote that the trend of frequency increase/decrease in the future experiment are statistically significant (95% level). Focusing on the global frequency, it is noteworthy that the maximum surface wind speeds, in the present simulation, are generally lower than those that are observed. The model is likely to underestimate the surface wind speeds and, therefore, the intensity of the tropical cyclones. The discrepancy may originate from some insufficient performance of the physical schemes in the 20 km-mesh model, including the cumulus parameterization. Originally formulated and incorporated in a coarser-mesh (e.g., T42, which is equivalent to horizontal mesh at a few 100 s of kilometers) version climate model, the physical schemes may fail to capture sufficient physical processes necessary for the tropical cyclone development. A considerable influence of the change in the physical processes upon tropical cyclone intensity, has also been suggested by other studies (e.g., Knutson and Tuleya 2004). To clarify the critical problem, detailed analyses on the interactions among the grid-scale physical processes, and subgrid-scale cumulus-scale processes, are necessary.

The findings will be discussed in a future article.

Here, the focus is on the comparison of the wind speeds between the present and future experiments. It is evident in Fig. 4 that the simulated change in the number of tropical cyclone occurrences in the globe is different in tropical cyclones of intense (>43 m s^{-1}), and weak-to-moderate (<43 m s^{-1}) classes. In the future experiment, tropical cyclones of the intense class increase in number, while those of weak-to-moderate class decline. In particular, the statistically significant (at 95% confidence level) increase is found for the class of 45–60 m s^{-1}. A similar contrasting trend of frequency change in the "weak-to-moderate" and "intense" class is equal across most of the ocean basins (not shown), though detailed estimates of its statistical significance may require a larger sampling number; the current result is highly dependent on the variance in the number sampled among the basins (Fig. 2, Table 1). The result is consistent with the finding from a lower-resolution (T106) GCM (Yoshimura et al. 2006) for the frequency change, and from the regional model (Knutson et al. 1998), in that the more intense tropical cyclones are likely to increase under the greenhouse-warmed climate.

To understand the quantitative difference in the maximum surface wind speeds of intense tropical cyclones, between the present-day and future experiments, we have monitored the largest maximum surface wind speed attained throughout the lifetime of all the tropical cyclones in the respective regions in respective years, and then calculated those statistics for 10 years. Table 2a contains the results from a comparison of the largest maximum surface wind speed in the present-day experiment with that from the future experiment. Aggregated over the globe, and over each hemisphere, the most intense tropical cyclones in the future experiment tend to become much stronger than those in the present-day experiment. In particular, at the statistical significance level of more than 95%, the increase is 6.7 m s^{-1} over the globe, 7.3 m s^{-1} in the Northern Hemisphere, and 8.7 m s^{-1} in the North Atlantic Ocean. The tendency is almost the same in the Southern Hemisphere. On a regional basis, this increase only occurs in the North Atlantic (95% significance) and South Indian (90% significance) basins. A significant (95% level) decrease occurs in the South Pacific, and the remaining basins have decreases which are not statistically significant. The tendency, including a sign of change, is basically true for the annual mean maximum wind speed averaged over all the simulated tropical cyclones in each region, except for the western North Pacific and the eastern North Pacific.

The discussion regarding the tropical cyclone intensity up to here has been devoted to the maximum wind speed. One might argue that the model may have trouble in simulating very strong wind speeds, but nonetheless can simulate fairly low surface pressure of tropical cyclone, and vice versa. To look briefly into this, we examine the relationship between the minimum surface pressure and the maximum surface wind of the simulated tropical cyclones in our model. The results are shown in Fig. 5, in which scattered diagrams of both physical variables are shown for (left) present-day experiment and (right) warmed climate experiment. Superimposed on both diagrams is a nonlinear regression line that specifies a relationship between minimum sea level pressure and maximum sustained wind speed derived from the observation of tropical cyclones in the western North Pacific (Atkinson and Holliday 1977). It seems that the range of scattered plots of the simulated maximum wind speeds and surface pressure in both experiments fit reasonably well into the regression line. In addition, we can see clear expansion of the surface pressures to lower values in the future experiment. This may demonstrate a reasonable performance of the present model in simulating tropical cyclones. On the other hand, it is noted that the model does not simulate central pressures nearly as low as observed in nature (down to 870 hPa). It appears that the lowest pressure is about 932 hPa in the present experiment, and about 912 hPa in the future experiment. We should note, however, that the observationally derived regression line probably contains uncertainty in the measurement, and careful interpretation may be needed for full exploration of the problem.

3.5 Seasonal variation of intensity

In this subsection, the target of the intensity comparison of the tropical cyclone between the

Table 2 Maximum surface wind speed (m s^{-1}) of TCs in the present-day and the future experiments. The two-sided Student's *t*-test was applied to the difference between the values of the two experiments. Standard deviations and percent changes are shown in parentheses. (a) For each year of the integrations, the maximum surface wind speed attained in the lifetime of all the TCs was selected, and the values for 10 years were then averaged. (b) The maximum surface wind speed attained in the lifetime of each TC was selected, and the values of all the TCs were averaged for each year of the integrations. The values for 10 years were then averaged.

(a) Annual maximums	Present 10 years Ave. (SD)	Future 10 years Ave. (SD)	F minus P (% change)
Global	49.3 (2.2)	56.0 (5.3)	6.7 (13.7) ###
Northern Hemisphere	47.0 (5.4)	54.2 (6.4)	7.3 (15.5) ##
Southern Hemisphere	47.6 (2.3)	50.8 (4.5)	3.3 (6.9) #
North Indian Ocean	30.2 (9.7)	25.2 (14.6)	−5.0 (−16.7)
Western North Pacific Ocean	45.8 (5.0)	44.8 (12.0)	−0.9 (−2.0)
Eastern North Pacific Ocean	39.9 (4.6)	37.9 (7.8)	−2.0 (−5.0)
North Atlantic Ocean	43.4 (7.1)	52.2 (4.9)	8.7 (20.1) ##
South Indian Ocean	46.5 (2.7)	50.3 (5.0)	3.8 (8.2) #
South Pacific Ocean	44.0 (3.7)	34.1 (9.9)	−9.9 (−22.5)**

(b) Annual averages	Present 10 years Ave. (SD)	Future 10 years Ave. (SD)	F minus P (% change)
Global	24.0 (1.0)	26.5 (1.8)	2.6 (10.7) ###
Northern Hemisphere	23.1 (1.4)	25.1 (2.2)	2.0 (8.5) #
Southern Hemisphere	25.0 (1.6)	28.5 (2.9)	3.5 (14.1) ###
North Indian Ocean	21.8 (7.2)	19.0 (5.3)	−2.8 (−12.8)
Western North Pacific Ocean	25.3 (2.9)	26.4 (5.2)	1.1 (4.2)
Eastern North Pacific Ocean	21.6 (2.0)	21.7 (3.3)	0.1 (0.6)
North Atlantic Ocean	28.1 (7.0)	31.2 (5.8)	3.1 (11.2)
South Indian Ocean	25.6 (1.6)	30.1 (3.5)	4.4 (17.3) ###
South Pacific Ocean	23.7 (2.9)	23.2 (4.3)	−0.5 (−2.0)

Statistically significant increase at 99% confidence level.
Statistically significant increase at 95% confidence level.
Statistically significant increase at 90% confidence level.
** Statistically significant decrease at 95% confidence level.
* Statistically significant decrease at 90% confidence level.

present-day and future experiments is shifted from the annually averaged trend to its seasonal (monthly) change. We investigate how the occurrence rate of the maximum wind speed of a tropical cyclone varies at different times of the year under a greenhouse-warmed condition when compared with the present-day condition. Figure 6 shows the occurrence rate of the maximum surface wind speeds from the (a) observation, (b) present-day experiment, and (c) future experiment, for all the simulated tropical cyclones for each experiment over the globe (GLOBAL) and in the Northern Hemisphere (NH), Southern Hemisphere (SH), North Indian Ocean (NI), and western North Pacific (WNP). The observational dataset used is the same as that described in Section 3.2. The occurrence rate is plotted in time-intensity coordinates, where the area integration spanning the panel equals 100%. Generally, the simulated seasonal change of the tropical cyclone occurrence rate in the present-day experiment agrees with our expectation, indicating a higher rate from July to September in the Northern

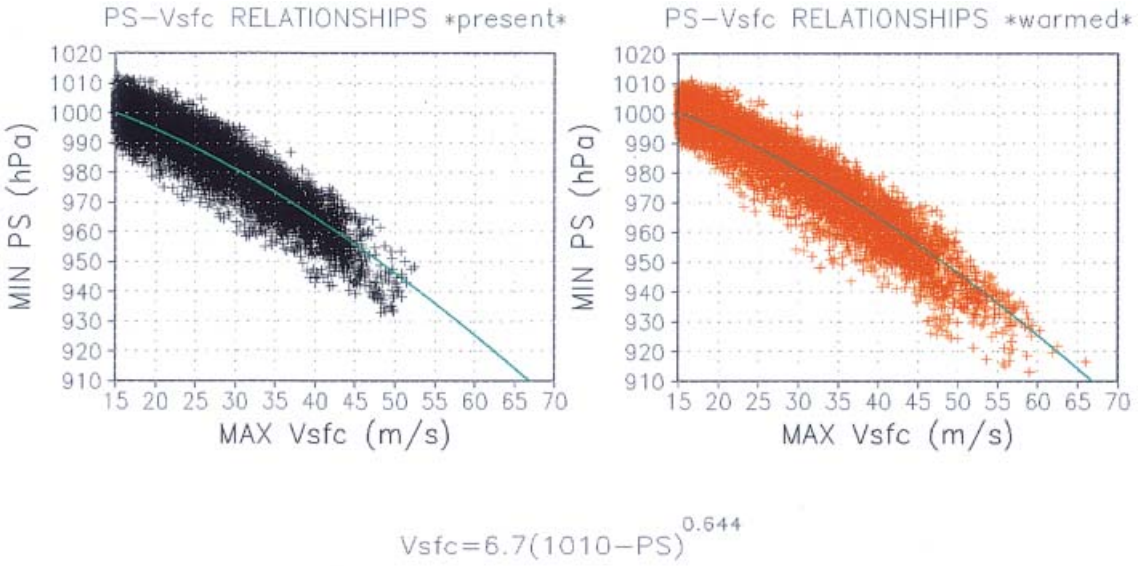

Fig. 5. Scattered diagram of minimum surface pressure versus maximum surface wind speed for all the simulated tropical cyclones in the (left) present-day experiment and (right) warmed climate experiment. Blue line is the nonlinear regression line of "surface wind (Vsfc in knot) and surface pressure (mb)" relationship from Atkinson and Holliday (1977).

Hemisphere and from January to March in the Southern Hemisphere. The pattern of the velocity range and the seasonal advance in the future experiment is remarkably similar to that in the present-day experiment; the tropical cyclones, with a higher rate of occurrence, still lie within the velocity range similar to that of the present-day experiment. A notable change is that the occurrence rate of the tropical cyclones with the maximum wind speed exceeding 50 m s^{-1} increases somewhat in the future experiment.

On hemispheric and basin scales, the simulated seasonality of the tropical cyclone activity varies from region to region. Broadly speaking, however, the comparison between the present-day experiment and observation reveals that the seasonal change of the simulated wind patterns is in agreement with the observation in the Northern Hemisphere, Southern Hemisphere, North Indian Ocean, and western North Pacific. We confirm that tropical cyclones are absent from June to September in the North Indian Ocean. The period is characterized by enhanced vertical shear around the region, due to the summer monsoon season, which tends to suppress the formation and development of tropical cyclones. Our model, thus, simulates the relevant basic climate of this region reasonably well (Kusunoki et al. 2005), demonstrating an improved representation of the seasonal change of the basic fields. On the other hand, in terms of the quantitative comparison, the model has a bias to simulate weaker wind speed compared to observation, which will be discussed later.

A comparison between the present-day and future experiments reveals no significant differences in the seasonal change of the occurrence rate aggregated over the globe (GLOBAL). However, one may notice that the monthly change in the pattern varies among the regions. Considering typhoons, for instance, which are a kind of tropical cyclone residing in the western North Pacific, the season usually ends in October in the present-day climate; however, in the future climate, the season usually continues until November. There is also an indication that intense typhoons (with a velocity exceeding 50 m s^{-1}), have a higher rate of occurrence from September to October. These changes should have something to do with the changes in the environmental conditions of tropical cyclones, a topic which will require further investigation.

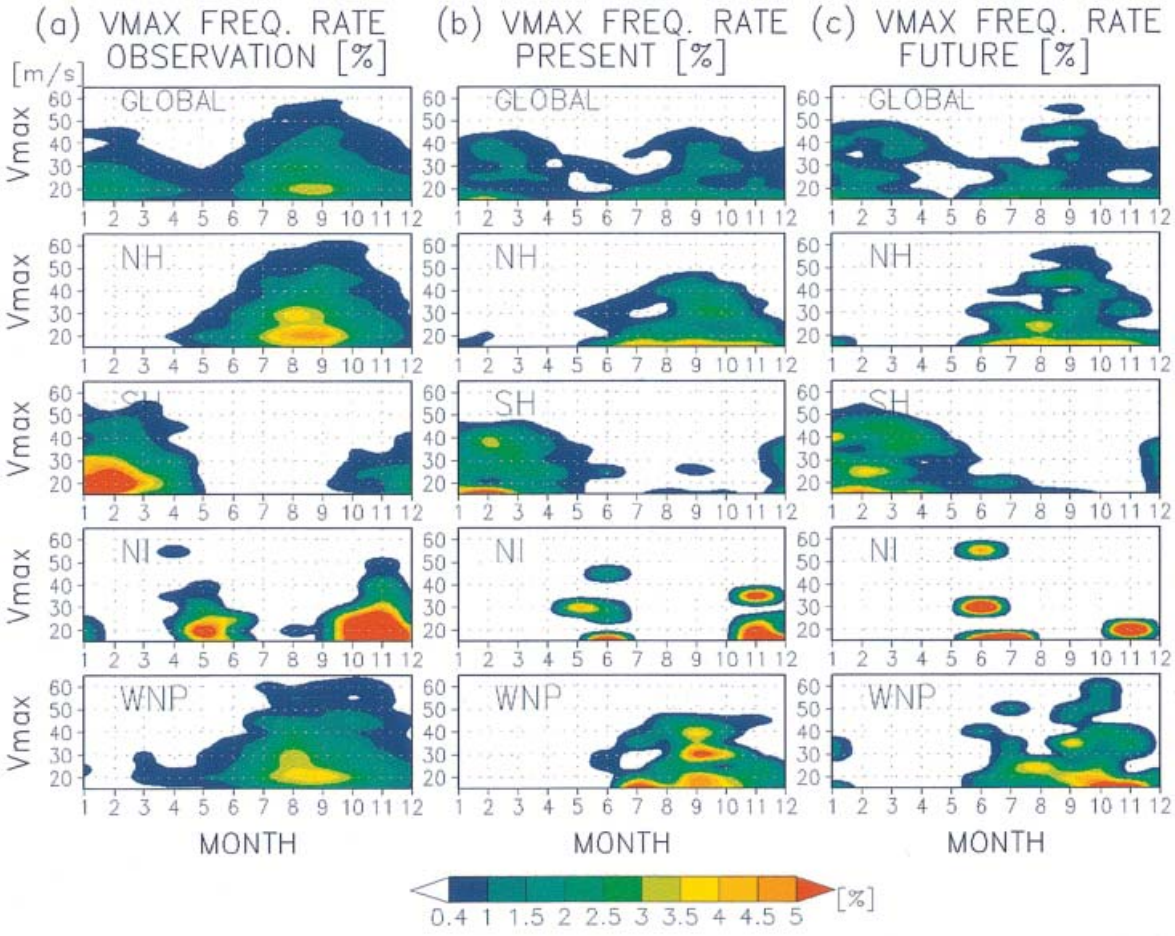

Fig. 6. Occurrence rate of the maximum surface wind speed of the tropical cyclones versus the month for (a) the observation, (b) the present-day experiment, and (c) the future experiment. The fractional rates (%) with respect to all the total tropical cyclones detected in the global (GLOBAL), Northern Hemisphere (NH), Southern Hemisphere (SH), North Indian Ocean (NI), and western North Pacific (WNP) regions are displayed.

4. Discussion and remarks

The previous studies using a global model with relatively high-resolution at that time (e.g., 100 km) suggested a general trend that the tropical cyclone frequency would be significantly reduced under the greenhouse-warmed environments (Bengtsson et al. 1996; Sugi et al. 2002). Yet, the resolution of the model was still insufficient to represent the typical inner structures of the observed tropical cyclone, and, partly for that reason, no general consensus on the suggested trend was achieved (IPCC 2001). It has been suggested from a theoretical line of thought, that an accurate representation of the intensity of a tropical cyclone requires a horizontal resolution that is fine enough to resolve the pressure gradients existing near the radius of the maximum winds (Persing and Montgomery 2005). In addition, a numerical simulation of a super typhoon, using a global model, indicated that high resolution is critical for representing the intense warm core in the inner rain area of a tropical cyclone (Krishunamurti and Oosterhof 1989). Thus, there has been a growing demand for a high-resolution climate model for studying the climatological aspects of future tropical cyclones. In the present study, the use of the 20 km-mesh climate model (AGCM), one of the highest-resolution models

of its kind, allows a reasonable representation of the inner structures of a tropical cyclone (Fig. 1), and may provide a more reliable projection of future tropical cyclones.

The results suggested that the frequency reduction of tropical cyclones is probable in the future, which supports findings from the previous studies. Though the mechanisms responsible for the frequency reduction under the future greenhouse-warmed condition are not fully understood, we infer that the stabilization of the atmosphere, caused by the greenhouse warming, could be a reason, as suggested by Knutson and Manabe (1995), Sugi et al. (2002), and Yoshimura et al. (2006). The inference is broadly supported by a comparison of the dry static stability between the future and present-day experiments; the future experiment shows an increase of approximately 10% more than that in the present-day experiment. The dry static stability here is defined as a difference in potential temperature between 250 hPa and the surface.

In terms of the intensity change, it appears that more intense tropical cyclones will increase in the future greenhouse-warmed climate. The finding is in agreement with previous studies using regional models (Knutson et al. 1998; Walsh and Ryan 2000; Knutson and Tuleya 2004) as well as a theoretical estimation using the thermodynamical factors relevant to tropical cyclone (Emanuel 1987; Holland 1997; Henderson-Sellers et al. 1998). The present study supports the finding in a more comprehensive manner, because of the long-term climate integration with the 20 km-mesh models. Another advantage of our model in coping with this problem would be that the dynamical effects of the environmental flow of a tropical cyclone, including the effect of vertical shear, might be represented consistently throughout the integration period. This feature should be checked in a future study. The importance of the effects in assessing the influence of global-warming upon the intensity of tropical cyclones was suggested by Walsh and Ryan (2000), but these effects have not been incorporated in most of the past modeling studies. Knutson and Tuleya (1999) suggested that the tropical cyclone, in the global warming environment, will be more intense in all the ocean basins, a suggestion which is at odds with our finding that the manner of change is basin-dependent. A reason for the discrepancy may be relevant to the absence of environmental dynamical effects on the tropical cyclones in their model.

It is noteworthy that the downscaling from low to high (fine) resolution AGCM alone does not resolve all the problems around accurate tropical cyclone projection. Even in the context of climate statistics, the model still has some shortcomings in capturing the observed geographical distribution, frequency, and intensity of a tropical cyclone. In particular, the deficiency of the intense (e.g., high wind speed of more than 60 m s^{-1}) tropical cyclone in our model was the most notable unanticipated result; however, the reasons are complex and difficult to understand. There are other issues to be clarified, which will make tropical cyclone projections more accurate and reliable. One may argue that the use of 20 km mesh is still coarse for representing the inner mesoscale structures of tropical cyclones. From another point of view, one may question the validity of the cumulus parameterization used in such a "high-resolution" hydrostatic model because moist process plays a key role in the development of tropical cyclones. It will be important to clarify the extent to which the cumulus parameterization, and other physical schemes are involved in the success of the current model. It will help clarify the caveats identified in our model including its bias for underpredicting the intensities of tropical cyclones when compared to observation. Since other physical parameterization schemes, such as a boundary layer treatment, should be of equal importance for improving the prediction of tropical cyclones, additional studies should be needed to clarify the intensity question.

This study does not treat some important questions concerning future tropical cyclone projection, which need to be investigated as a future work. First, this study does not fully investigate possible changes in the maximum central pressure of the future tropical cyclones, which is an important research theme to deepen our understanding on the characteristics of tropical cyclones in the future greenhouse-warmed climate. Also there remains a question of how the duration of tropical cyclone will change under a greenhouse-warmed climate.

This is also an important research topic. Evidence is emerging that the tropical cyclone activity in the past 30 years in the North Pacific and North Atlantic is increasing significantly, and that the storms are characterized by greater duration and intensity, which are attributed, at least partially, to anthropogenic activities (Emanuel 2005).

Even with these unresolved issues, the tropical cyclone projections with the 20 km-mesh climate model represent an advancement, and the general trend of tropical cyclones in the future greenhouse-warmed climate is represented to a reasonable degree and justified as follows. First, extreme events other than the tropical cyclone, including the Baiu front, have been reproduced reasonably well with the model (Kusunoki et al. 2005), along with the successful representation of long-term averaged climatology (Mizuta et al. 2006). Furthermore, the experiments have been used to provide some boundary conditions for the nonhydrostatic regional modeling of an Asian monsoon at 5 km mesh, and these conditions turned out to work well in the nonhydrostatic model (Yoshizaki et al. 2005). Thus, the model suitably reproduces the fundamental climate features and attendant larger-scale background disturbances of tropical cyclones. Second, the spontaneous development of a tropical cyclone with a typical inner structure (eye, eyewall-like, and spiral-bank-like structures) is represented to a more realistic extent in a hydrostatic modeling framework. To understand a genesis process of the tropical cyclones, a challenging and appealing issue, remains to be attempted in the present work, and will be investigated in a future work. It is our opinion that the major advancement from the past AGCM studies is that the tropical cyclone, including its inner structures, is represented not as a result of some artificially forcing or seeding from initial disturbances but, rather, as a result of its spontaneous interaction with environmental disturbances throughout the 10-year integration period. From a 16-day integration of a 10 km-mesh global hydrostatic model on the Earth Simulator, Ohfuchi et al. (2004) reported that the model is capable of representing the typical mesoscale convective structure of a typhoon (tropical cyclone residing in and around the North Pacific) reasonably well. From a similar line of reasoning, but based on the time integration and analysis spanning a global and climate scale, our strategy of using a 20 km-mesh hydrostatic model is appropriate for the representation of the convective structure of a tropical cyclone that develops and decays in a climate system. The results reported in this article are expected to provide further insights into a potentially more reliable projection of future tropical cyclone climatology.

Acknowledgments

The calculations were performed on the Earth Simulator as a part of the project RR2002, "Development of Super-High-Resolution Global and Regional Climate Models," funded by the Ministry of Education, Culture, Sports, Science, and Technology (MEXT), Japan. Relevant subproject members, other than the authors of this article, include T. Aoki, M. Hosaka, H. Ishizaki, A. Kitoh, T. Matsuo, T. Shibata, T. Uchiyama, T. Yasuda, and S. Yukimoto (Meteorological Research Institute, MRI), M. Hirai, T. Hosomi, T. Kadowaki, K. Katayama, H. Kawai, M. Kazumori, H. Kitagawa, C. Kobayashi, M. Kyoda, S. Maeda, T. Matsumura, S. Murai, M. Nakagawa, A. Narui, T. Ose, R. Sakai, T. Sakashita, Y. Takeuchi, K. Yamada, and M. Yamaguchi (Japan Meteorological Agency, JMA), and K. Fukuda, K. Horiuchi, K. Miyamoto, and H. Murakami (Advanced Earth Science & Technology Organization, AESTO), all in alphabetical order. The timely and thoughtful comments on the research by Prof. Akio Arakawa and Drs. Tatsushi Tokioka and Kozo Ninomiya are acknowledged. Last but not the least, the authors would like to thank two anonymous referees for their insightful and constructive comments on the original manuscript.

References

Arakawa, A. and W.H. Schubert, 1974: Interaction of cumulus cloud ensemble with the large-scale environment. Part I. *J. Atmos. Sci.*, **31**, 674–701.

Atkinson, G.D. and C.R. Holliday, 1977: Tropical cyclone minimum sea level pressure/maximum sustained wind relationship for the western North Pacific. *Mon. Wea. Rev.*, **105**, 421–427.

Bengtsson, L., M. Botzet, and M. Esch, 1996: Will greenhouse gas-induced warming over the next 50 years lead to higher frequency and greater intensity of hurricanes? *Tellus*, **48A**, 57–73.

———, 2001: Huricane threats. *Science*, **293**, 440–441.

Broccoli, A.K. and S. Manabe, 1990: Can existing climate models be used to study anthropogenic changes in tropical cyclone climate? *Geophys. Res. Lett.*, **17**, 1917–1920.

Camargo, S.J. and A.H. Sobel, 2004: Formation of tropical storms in an atmospheric general circulation model. *Tellus*, **56A**, 56–67.

———, A.G. Barnston, and S.E. Zebiak, 2005: A statistical assessment of tropical cyclone activity in atmospheric general circulation models. *Tellus*, **57A**, 589–604.

Chang, C.-P., C.-H. Liu, and H.-C. Kuo, 2003: Typhoon Vamei: An equatorial tropical cyclone formation. *Geophys. Res. Lett.*, **30**, No. 3, 1150, doi:10.1029/2002GL016365.

Emanuel, K.A., 1987: The development of hurricane intensity on climate. *Nature*, **326**, 483–485.

———, 2005: Increasing destructiveness of tropical cyclones over the past 30 years. *Nature*, **438**, 686–688.

Haarsma, R.J., J.F.B. Mitchell, and C.A. Senior, 1993: Tropical disturbances in a GCM. *Clim. Dyn.*, **8**, 247–257.

Henderson-Sellers, A. and Coauthors, 1998: Tropical cyclones and global climate change: A post-IPCC assessment. *Bull. Amer. Meteor. Soc.*, **79**, 19–38.

Holland, G.J., 1997: The maximum potential intensity of tropical cyclones. *J. Atmos. Sci.*, **54**, 2519–2541.

IPCC (Intergovernmental Panel on Climate Change), *Special Report on Emissions*. A Special Report of Working Group III of the Intergovernmental Panel on Climate Change. Cambridge University Press, Cambridge, UK (2000).

IPCC (Intergovernmental Panel on Climate Change), *Climate Change 2001: The Scientific Basis. Contribution of Working Group I to the Third Assessment Report of the Intergovernmental Panel on Climate Change*. Cambridge University Press, United Kingdom and New York, NY, USA, 881pp.

Kang, L.S., K. Jin, B. Wang, K.M. Lau, J. Shukla, V. Krishnamurthy, S.D. Schubert, D.E. Waliser, W.F. Stern, A. Kitoh, G.A. Meehl, M. Kanamitsu, V.Y. Galin, V. Satyan, C.K. Park, and Y. Liu, 2002: Intercomparison of the climatological variations of Asian summer monsoon precipitation simulated by 10 GCMs. *Clim. Dyn.*, **19**, 383–395.

Knutson, T.R. and S. Manabe, 1995: Time-mean response over the tropical Pacific to increased CO2 in a coupled ocean-atmosphere model. *J. Climate*, **8**, 2181–2199.

———, R.E. Tuleya, and Y. Kurihara, 1998: Simulated increase of hurricane intensities in a CO2-warmed climate. *Science*, **279**, 1018–1020.

——— and R.E. Tuleya, 1999: Increased hurricane intensities with CO2-induced warming as simulated using the GFDL hurricane prediction system. *Clim. Dyn.*, **15**, 503–519.

——— and ———, 2004: Impact of CO2-Induced warming on simulated hurricane intensity and precipitation: Sensitivity to the choice of climate model and convective parameterization. *J. Climate*, **17**, 3477–3495.

Krishnamurti, T.N. and D.K. Oosterhof, 1989: Prediction of the life cycle of a supertyphoon with a high-resolution global model. *Bull. Amer. Meteor. Soc.*, **70**, 1218–1230.

———, ———, and N. Dignon, 1989: Hurricane Prediction with a high resolution global model. *Mon. Wea. Rev.*, **117**, 631–669.

———, R. Correa-Torres, M. Latif, and G. Daughenbaugh, 1998: The impact of current and possibly future sea surface temperature anomalies on the frequency of Atlantic hurricanes. *Tellus*, **50A**, 186–210.

Kusunoki, S., J. Yoshimura, H. Yoshimura, A. Noda, K. Oouchi, and R. Mizuta, 2005: Change of Baiu in global warming projection by an atmospheric general circulation model with 20-km grid size. *J. Meteor. Soc. Japan*. (Submitted.)

Mizuta, R., K. Oouchi, H. Yoshimura, A. Noda, K. Katayama, S. Yukimoto, M. Hosaka, S. Kusunoki, H. Kawai, and M. Nakagawa, 2006: 20 km-mesh global Climate simulations using JMA-GSM model. *J. Meteor. Soc. Japan*, **84**, 165–185.

Ohfuchi, W., H. Nakamura, M.K. Yoshioka, T. Enomoto, K. Takaya, X. Peng, S. Yamane, T. Nishimura, Y. Kurihara, and K. Ninomiya, 2004: 10-km mesh meso-scale resolving simulations of the global atmosphere on the Earth Simulator—preliminary outcomes of AFES (AGCM for the Earth Simulator)—. *J. Earth Simulator*, **1**, 8–34.

Persing, J. and M.T. Montgomery, 2005: Is environmental CAPE important in the determination of maximum possible hurricane intensity? *J. Atmos. Sci.*, **62**, 542–550.

Pezza, A.B. and I. Simmonds, 2005: The first South Atlantic hurricane: Unprecedented blocking, low shear and climate change. *Geophys. Res. Lett.*, **32**, L15712, doi:10.1029/2005GL023390.

Randall, D.A. and D.M. Pan, 1993: Implementation of the Arakawa-Schubert cumulus parameterization with a prognostic closure. The Representation of Cumulus Convection in Numerical Models, *Meteor. Monogr., Amer. Meteor. Soc.*, **46**, 137–144.

Sato, T., 2004: The current status of the Earth Simulator. *J. Earth Simulator*, **1**, 6–7.

Sugi, M., A. Noda, and N. Sato, 2002: Influence of the global warming on tropical cyclone climatology: An experiment with the JMA global model. *J. Meteor. Soc. Japan*, **80**, 249–272.

Tsutsui, J., 2002: Implications of anthropogenic climate change for tropical cyclone activity: A case study with the NCAR CCM2. *J. Meteor. Soc. Japan*, **80**, 45–65.

Walsh, K.J.E. and B.F. Ryan, 2000: Tropical cyclone intensity increase near Australia as a result of climate change. *J. Climate*, **13**, 3237–3254.

Webster, P.J., G.J. Holland, J.A. Curry, and H.-R. Change, 2005: Changes in tropical cyclone number, duration, and intensity in a warming environment. *Science*, **309**, 1844–1846.

Willoughby, H.E., F.D. Marks Jr., and R.J. Feinberg, 1984: Stationary and moving convective bands in hurricanes. *J. Atmos. Sci.*, **41**, 3189–3211.

Yoshimura, H. and T. Matsumura, 2003: A semi-Lagrangian scheme conservative in the vertical direction. CAS/JSC WGNE *Research Activities in Atmospheric and Ocean Modeling*, **33**, 3.19–3.20.

——— and ———, 2005: A two-time-level vertically-conservative semi-Lagrangian semi implicit double Fourier series AGCM. CAS/JSC WGNE *Research Activities in Atmospheric and Ocean Modeling*, **35**, 3.27–28.

——— and ———, 2004: A vertically conservative two-time-level semi-Lagrangian semi-implicit scheme. The 2004 Workshop on the Solution of Partial Differential Equations on the Sphere. Yokohama.

Yoshimura, J., M. Sugi, and A. Noda, 2006: Influence of greenhouse warming on tropical cyclone frequency. *J. Meteor. Soc. Japan*, **84**, 405–428.

Yoshizaki, M., C. Muroi, S. Kanada, Y. Wakazuki, K. Yasunaga, A. Hashimoto, T. Kato, K. Kurihara, A. Noda, and S. Kusunoki, 2005: Changes of Baiu (Mei-yu) frontal activity in the global warming climate simulated by a non-hydrostatic regional model. *SOLA*, **1**, 25–28.

Yukimoto, S., A. Noda, A. Kitoh, M. Hosaka, H. Yoshimura, T. Uchiyama, K. Shibata, O. Arakawa, and S. Kusunoki, 2006: Present-Day Climate and Climate Sensitivity in the Meteorological Research Institute Coupled GCM, Version 2.3 (MRI-CGCM2.3). *J. Meteor. Soc. Japan*, **84**, 333–363.

Note: After submitting the final version of this article, the authors noticed that Webster et al. (2005) provided a significant, new observational evidence for emergence of global upward trend in tropical cyclone intensity based on an observational dataset of 35-year period. The trend is consistent with our major findings.